



A dynamic collision avoidance solution scheme of unmanned surface vessels based on proactive velocity obstacle and set-based guidance

Wang Wenming^a, Du Jialu^{b,*}, Tao Yihan^b

^a School of Marine Engineering, Dalian Maritime University, Dalian, 116000, China

^b School of Marine Electrical Engineering, Dalian Maritime University, Dalian, 116000, China

ARTICLE INFO

Keywords:

Unmanned surface vessel
COLREGs
Proactive velocity obstacle
LOS method
Set-based guidance
Dynamic collision avoidance

ABSTRACT

This paper proposes a proactive velocity obstacle (PVO) method through pre-judging whether there are collision risks between an unmanned surface vessel (USV) and its obstacle vessels according to the predicted motion states of the USV by its motion mathematical model to optimize the collision avoidance decision-making. Then integrating the proposed PVO method and the line of sight (LOS) algorithm into the set-based guidance (SBG) framework, we create a dynamic collision avoidance (DCA) solution scheme of USVs and carry out simulations in the cases of single vessel and multiple vessels encounter, respectively. The USV-DCA solution scheme can make the USV successfully avoid obstacle vessels while complying with the international regulations for preventing collisions at sea (COLREGs) and follow the desired path without collisions. The simulation results show that the USV-DCA solution scheme based on PVO and SBG can make USVs avert a series of small velocity changes and make a safer collision avoidance decision than the original SBG framework scheme in the multiple vessels encounter case, which verifies the effectiveness and superiority of our proposed USV-DCA solution scheme.

1. Introduction

Unmanned surface vessels (USVs) (Cheng et al., 2019) refer to intelligent transportation platforms that can navigate autonomously depending on shipboard navigation system. In complex and changing marine environment, an important premise for the safe navigation of USVs is that they can autonomously navigate with collision avoidance (Xu et al., 2020). In 2018, Ministry of Industry and Information Technology, Ministry of Transport and State Administration of Science, and Technology and Industry for National Defense of the People's Republic of China jointly drew up "Execution Plan for Intelligent Ship Development (2019–2021)", where it is clearly proposed that the collision avoidance technology ought to be broken through as soon as possible (MIIT, 2019). The international regulations for preventing collisions at sea (COLREGs) formalized by International Maritime Organization (IMO) also require proactive actions made to avoid collision (IMO, 1972), which means that USVs should autonomously make decisions to achieve the goal of collision avoidance.

Since USVs inevitably encounter with a single vessel or multiple vessels during navigation in the ocean, more attentions are paid to the problem of collision avoidance with dynamic obstacle vessels of USVs.

Many method, such as artificial potential field (APF) (Khatib, 1986), dynamic window (DW) (Fox and Burgard, 1997) and velocity obstacle (VO) (Fiorini and Shiller, 1998), have been applied to locally dynamic collision avoidance of USVs. Naeem et al. (2016) used the APF method to make USVs avoid obstacles in the ocean and navigate to the target point with help of the attraction potential and repulsive potential functions, however, this method tends to fall into the local optimal solutions (Song et al., 2018). Loe (2008) proposed a modified-DWA-based collision avoidance method for autonomous surface vessels (ASVs), which considered vessels dynamics and made the collision avoidance behavior of ASVs comply with COLREGs. However, it is computationally heavy. Fortunately, the VO method is simple to compute and easy to adapt and tune for different collision avoidance requirements (Moe and Pettersen, 2016; Kufoalor et al., 2018).

The VO method was firstly proposed for the collision avoidance of mobile robots in (Fiorini and Shiller, 1998), and then its various variations, such as reciprocal VO (Berg et al., 2008) and probabilistic VO (Kluge and Prassler, 2004) methods, were proposed for different collision avoidance problems. The VO method finds all velocities at which a robot will collide with any obstacle some time in the future and these velocities form a cone-like area which is called the velocity obstacle

* Corresponding author.

E-mail address: dujl66@163.com (D. Jialu).

cone. Collisions will definitely be avoided if the robot moves at a velocity outside of this cone. In recent years, the VO method has been used to solve the collision avoidance problem of surface vessels. Kuwata et al. (2014) used the VO method to guarantee a collision-free and COLREGs-complying trajectory of a USV by maintaining a velocity outside of the velocity obstacle cone. Zhao et al. (2016) first evaluated collision risks between a USV and its obstacle vessels using evidential reasoning theory, and then made the decision about the optimal collision avoidance velocity of USVs using the VO method. Sandbakken (2018) respectively used the VO and APF methods to make collision-avoiding decisions for a cargo vessel during the ocean transportation, the simulation results show that the VO method is easier to achieve the collision avoidance target under the premise of complying with COLREGS than the APF method. However, the references (Kuwata et al., 2014; Zhao et al., 2016; Sandbakken, 2018) assume that the velocity of vessels is instantaneously and linearly changing and do not consider the dynamic characteristics of the vessel motion. These problems may cause a series of small velocity changes of USVs, which results in the decrease of the collision avoidance performance and non-compliance with the good seamanship requirement of COLREGS. Considering the dynamic characteristics of mobile robots, the references (Alonso-Mora et al., 2013a,b) used the VO method to obtain a more realistic optimal collision avoidance velocity for the robot.

On the other hand, to plan and control the motion of surface vessels under collision avoidance, a guidance, navigation and control (GNC) system is required, where the guidance subsystem continuously computes the reference position and velocity or acceleration of marine vessels to be used by the motion control subsystem (Fossen, 2011). In 2016, Moe and Pettersen (2016) proposed a set-based guidance (SBG) framework to implement the autonomous navigation of USVs, where path following and collision avoidance are regarded as USVs' two separate tasks that are switched according to the actual distance between a USV and its obstacle vessels such that the USV can navigate along the desired path while avoiding collisions with static and dynamic obstacles. However, therein the safe-radius-following (SRF) collision avoidance method has limitations in the multiple vessels encounter cases, that is, it results in a passive collision avoidance decision-making and even potential collision avoidance failure in the multiple vessels

decision-making; further, we create a dynamic collision avoidance (DCA) solution scheme of USVs by integrating the proposed PVO method and the line of sight (LOS) algorithm into the SBG framework, which can increase the autonomy and safety of USVs' collision avoidance process in the cases of single vessel or multiple vessels encounter. And our proposed scheme is easy to implement in engineering.

This paper is organized as follows: The mathematical model of USVs and the research objective are given in Section 2. The VO method is improved in Section 3 and the USV-DCA solution scheme based on PVO and SBG is designed in Section 4. Section 5 presents the simulation results and Section 6 concludes this paper.

2. Vessel model and research objective

The motion mathematical model of an underactuated USV is expressed as follows (Fossen, 2011).

$$\begin{cases} \dot{\eta} = J(\psi)v \\ M\ddot{v} + C(v)v + D(v)v = \tau \end{cases} \quad (1)$$

where $\eta = [x, y, \psi]^T$ comprising of a USV's position (x, y) and course ψ in the north-east frame; $v = [u, v, r]^T$ denotes velocities of a USV consisting of velocities u in surge, v in sway and r in yaw in the body-fixed frame, respectively; $\tau = [\tau_u, 0, \tau_r]^T$ denotes the actual control vector consisting of surge force τ_u and yaw moment τ_r ; $J(\psi)$ denotes the rotation matrix; M is the symmetric and positive-definite inertia matrix with the added mass; $C(v)$ is the Coriolis and centripetal matrix; $D(v)$ is the hydrodynamic damping matrix. They are

$$J(\psi) = \begin{bmatrix} \cos\psi & -\sin\psi & 0 \\ \sin\psi & \cos\psi & 0 \\ 0 & 0 & 1 \end{bmatrix}$$

$$M = \begin{bmatrix} m_{11} & 0 & 0 \\ 0 & m_{22} & m_{23} \\ 0 & m_{32} & m_{33} \end{bmatrix}$$

$$C(v) = \begin{bmatrix} 0 & 0 & -m_{22}v - m_{23}r \\ 0 & 0 & m_{11}u \\ m_{22}v + m_{23}r & -m_{11}u & 0 \end{bmatrix} \quad D(v) = \begin{bmatrix} X_{u1} + \sum_{i=2}^3 X_{ui}|u|^{i-1} & 0 & 0 \\ 0 & Y_{v1} + \sum_{i=2}^3 Y_{vi}|v|^{i-1} & 0 \\ 0 & 0 & N_{r1} + \sum_{i=2}^3 N_{ri}|r|^{i-1} \end{bmatrix}$$

encounter cases.

Motivated by the aforementioned literature, we innovatively proposed the proactive VO (PVO) method which can pre-judge whether there are collision risks according to the predicted position and velocity of USVs by its motion mathematical model, hence make USVs avert a series of small velocity changes, and optimize the collision avoidance

where $m_{11} = m - X_{\dot{u}}$, $m_{22} = m - Y_{\dot{v}}$, $m_{23} = mx_g - Y_{\dot{r}}$, $m_{32} = mx_g - Y_{\dot{r}}$, $m_{33} = I_z - N_{\dot{r}}$, m is the mass of the USV, x_g denotes the longitudinal position of the gravity center of the vessel relative to the body-fixed frame; I_z is the moment of inertia in yaw, $X_{(\bullet)}$, $Y_{(\bullet)}$, $N_{(\bullet)}$ are the hydrodynamic coefficients.

The research objective in this paper is to create a DCA solution

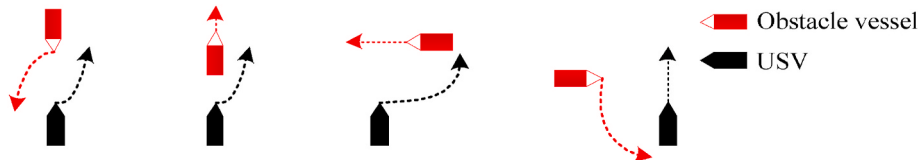


Fig. 1. Typical encounter scenarios.

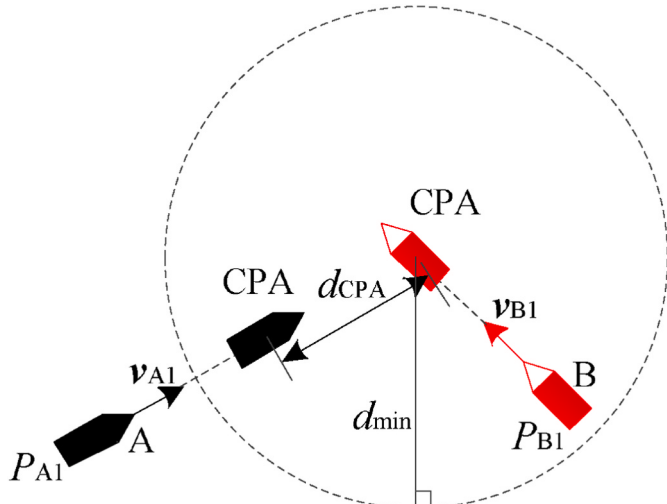


Fig. 2. The schematic diagram of the crossing encounter.

scheme of USVs, specifically, to design a guidance and control system of a USV such that the USV can navigate along the desired path while avoiding collisions with other obstacle vessels under complying with COLREGs. Here, collision avoidance should and must have the highest priority so as to guarantee a safe navigation of the USV if there are any obstacles around the USV. The research objective is formalized in order of priority as follows :

- In order to avoid collisions, it is required that the distance between the USV and any obstacle vessel always be greater than or equal to a safe distance d_{\min} :

$$|P(t) - P_O(t)| \geq d_{\min}, \forall t \geq 0 \quad (2)$$

where $P(t)$ is the position of the USV and $P_O(t)$ is the position of any obstacle vessel.

- The USV position should follow the desired path, i.e.

$$\lim_{t \rightarrow \infty} y_e(t) = 0 \quad (3)$$

where y_e is the path cross-track error defined as the shortest distance between the USV and any point on the path. $y_e = 0$ implies that the USV is on the path.

3. PVO method

3.1. COLREGs about Steering and sailing

The rules 13–15 about steering and sailing in the part B of COLREGs (IMO, 1972) respectively describe how a vessel should act to avoid collision with an obstacle vessel in head-on, overtaking and crossing encounter scenarios, as shown in Fig. 1. The rule 8 about steering and sailing describes the following detailed requirements about actions to avoid collision.

- Actions taken to avoid collision should be positive if the circumstances admit.
- Any alterations of course and/or speed to avoid collision shall be large enough to be apparent to another vessel, where the course represents the angle of the velocity and the speed represents the magnitude of the velocity; A series of small alterations of course and/or speed should be avoided.
- Course changes may be the most effective action to avoid collision if the sea area is large enough.

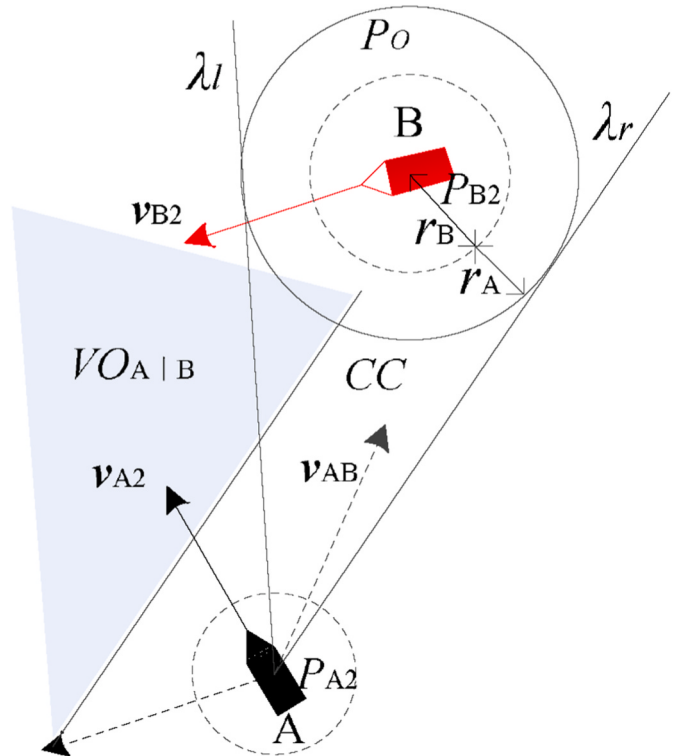


Fig. 3. The schematic diagram of a velocity obstacle.

- Actions taken to avoid collisions with another vessel shall result in the USV navigate around the obstacle vessel at a safe distance.

3.2. Conditions and velocity obstacles to avoid collisions

There are two vessels named A and B, respectively, in Fig. 2. At the moment, the vessel A is at the position P_A1 and is sailing at the velocity v_{A1} ; the vessel B is at the position P_{B1} and is sailing at the velocity v_{B1} ; when the distance between the vessels A and B is minimal, the positions where the two vessels are located are called the closest points of approach (CPA) to each other, as shown in Fig. 2. This minimum distance is represented by d_{CPA} , called the distance at CPA; the time for the vessel A to arrive from the position P_A1 to the CPA is represented by t_{CPA} , called the time to CPA. The two parameters d_{CPA} and t_{CPA} can be respectively calculated by the following formulas (Kuwata et al., 2014).

$$\begin{cases} t_{\text{CPA}} = \frac{(\mathbf{P}_B - \mathbf{P}_A) \cdot (\mathbf{v}_A - \mathbf{v}_B)}{\|\mathbf{v}_A - \mathbf{v}_B\|^2} \\ d_{\text{CPA}} = \|(\mathbf{P}_A + \mathbf{v}_A \cdot t_{\text{CPA}}) - (\mathbf{P}_B + \mathbf{v}_B \cdot t_{\text{CPA}})\| \end{cases} \quad (4)$$

where \mathbf{P}_A and \mathbf{P}_B are the position vectors of the vessels A and B, respectively.

The vessels will have a collision risk if

$$0 \leq t_{\text{CPA}} \leq t_{\max} \text{ and } d_{\text{CPA}} \leq d_{\min} \quad (5)$$

where d_{\min} is the safe distance that complying with the rule 8-(iv) of COLREGs; t_{\max} is the tolerant latest time to take collision avoidance actions. d_{\min} is related to the size of the two vessels.

Now we construct velocity obstacles through the VO method. In Fig. 3, the vessel A represents a USV and the vessel B represents an obstacle vessel. At the moment, the vessel A is at the position P_A2 and is sailing at the velocity v_{A2} ; the vessel B is at the position P_{B2} and is sailing at the velocity v_{B2} , and they are in a crossing encounter scenario. As shown in Fig. 3, the two dotted-line circles surrounding the vessels A and B are defined as the vessel domains A and B, respectively. If any vessel

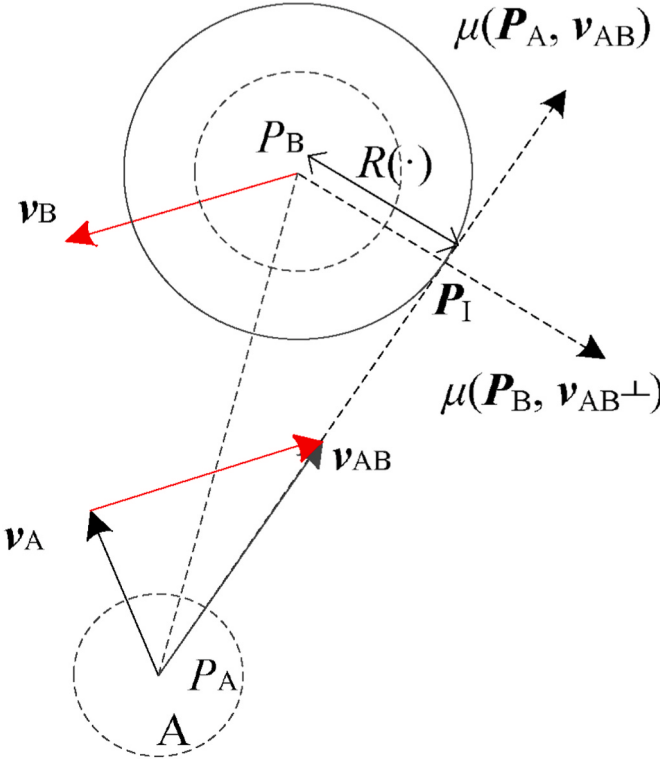


Fig. 4. Illustration for driving $R(P_B, \mu(P_A, \mathbf{v}_{AB})) = d_{CPA}$.

enters another vessel domain, the two vessels will have a high probability to collide, that is, the vessel domain represents a safe area for vessels not to collide. On the other hand, if the vessel domains of the two vessels intersect at a future moment, there will exist a collision risk. r_A and r_B represent the radius of the vessel domains A and B, respectively, and they meet

$$\begin{cases} r_A > \frac{l_A}{2}, r_B > \frac{l_B}{2} \\ r_B \geq d_{\min} - r_A \end{cases} \quad (6)$$

where l_A and l_B are the lengths of the vessels A and B, respectively.

We extend the radius of the vessel domain B from r_B to $r_B + r_A$, as shown in Fig. 3, and then relative to the solid-line circle with the radius $r_A + r_B$, the vessel A can be viewed as a mass point in its position P_A . The area which the solid-line circle encloses is defined as the position obstacle P_O ; λ_l and λ_r are two rays starting from the mass point P_A and being tangent to the solid-line circle; \mathbf{v}_{AB} is the velocity of the vessel A relative to the vessel B; λ_{AB} is a ray along the \mathbf{v}_{AB} direction starting from the mass point P_A . In the crossing encounter scenario, in order to avoid the collision with the vessel B, the vessel A should take appropriate actions complying with COLREGs, thus \mathbf{v}_A and \mathbf{v}_{AB} are changing. Some velocities of the vessel A relative to the vessel B may lead to collision risks between the two vessels. The set which these velocities form is defined as the collision cone (CC):

$$CC = \{\mathbf{v}_{AB} \mid \lambda_{AB} \cap P_O \neq \emptyset\} \quad (7)$$

Then we can construct a velocity obstacle $VO_{A|B}$ of the vessel A

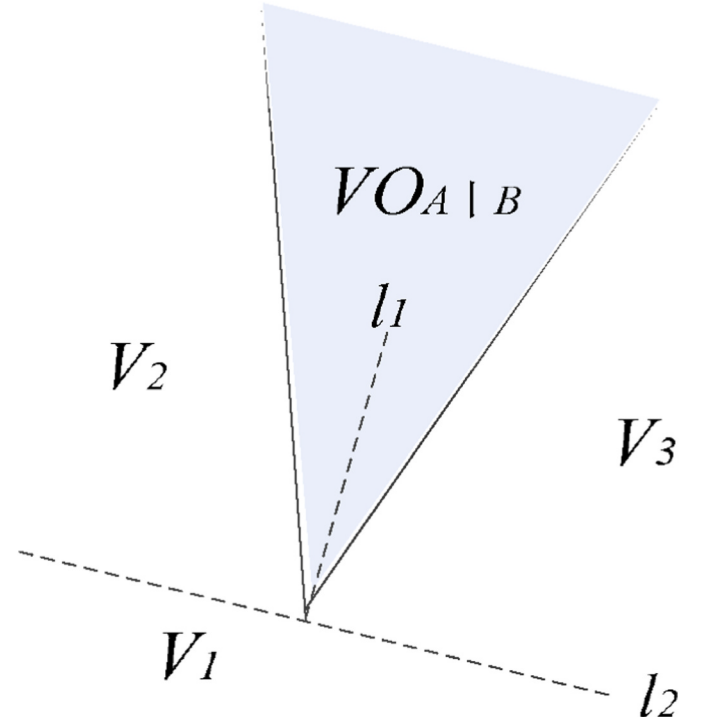


Fig. 5. Division of the velocity area.

caused by the vessel B through shifting the CC along the direction of \mathbf{v}_{B2} by the magnitude of \mathbf{v}_{B2} .

$$VO_{A|B} = \{\mathbf{v}_A \mid (\mathbf{v}_A - \mathbf{v}_B) \in CC \oplus \mathbf{v}_{B2}\} \quad (8)$$

where \oplus represents the Minkowski summing operator. $VO_{A|B}$ is a cone-like area, like the gray area shown in Fig. 3. Collisions will definitely be avoided if the vessel A navigates at a velocity outside of the $VO_{A|B}$. When there are n obstacle vessels around the vessel A, the total velocity obstacle TVO of the vessel A is

$$TVO = \bigcup_{i=1}^n VO_{A|i} \quad (9)$$

Choosing a velocity outside of the $VO_{A|B}$ for the USV, i.e., choosing a \mathbf{v}_{AB} outside of the CC, is equivalent to guaranteeing $d_{CPA} \geq d_{\min}$. Consider the encounter scenario in Fig. 3. Note that $\mu(\mathbf{P}, \mathbf{v}) = \{\mathbf{P} + t\mathbf{v} \mid t > 0\}$ to represent the ray starting from position P in the direction of \mathbf{v} . Here $R(\mathbf{P}_n, \mu(\mathbf{P}, \mathbf{v}))$ represents the radius of the circle with the center P_n , to which the ray $\mu(\mathbf{P}, \mathbf{v})$ is tangent.

As shown in Fig. 4, $\mu(\mathbf{P}_A, \mathbf{v}_{AB})$ is tangent to the circle C_R with the radius $R(\mathbf{P}_B, \mu(\mathbf{P}_A, \mathbf{v}_{AB})) = r_A + r_B$ and the center P_B . Make a ray $\mu(\mathbf{P}_B, \mathbf{v}_{AB}^\perp)$ starting from P_B in the direction perpendicular to \mathbf{v}_{AB} , which means that $\mu(\mathbf{P}_B, \mathbf{v}_{AB}^\perp)$ is perpendicular to $\mu(\mathbf{P}_A, \mathbf{v}_{AB})$, then their intersection P_I is a tangent point of the $\mu(\mathbf{P}_A, \mathbf{v}_{AB})$ to the circle C_R . If $\mu(\mathbf{P}_A, \mathbf{v}_{AB}) = \mu(\mathbf{P}_B, \mathbf{v}_{AB}^\perp) \Rightarrow \mathbf{P}_A + \mathbf{v}_{AB} \cdot t = \mathbf{P}_B + \mathbf{v}_{AB}^\perp \cdot t$, the time for a point to move at \mathbf{v}_{AB} from P_A to P_I is $t = \frac{(\mathbf{P}_B - \mathbf{P}_A)}{\mathbf{v}_{AB} - \mathbf{v}_{AB}^\perp} = \frac{(\mathbf{P}_B - \mathbf{P}_A) \cdot \mathbf{v}_{AB}}{(\mathbf{v}_{AB} - \mathbf{v}_{AB}^\perp) \cdot \mathbf{v}_{AB}} = \frac{(\mathbf{P}_B - \mathbf{P}_A) \cdot \mathbf{v}_{AB}}{\|\mathbf{v}_{AB}\|^2}$ which is the same as the t_{CPA} given by (4). Then it is obtained from Fig. 4 that

$$R(\mathbf{P}_B, \mu(\mathbf{P}_A, \mathbf{v}_{AB})) = \|\mathbf{P}_I - \mathbf{P}_B\| = \|(\mathbf{P}_I - \mathbf{P}_A) - \mathbf{P}_B + \mathbf{P}_A\| = \|(\mathbf{v}_A - \mathbf{v}_B) \cdot t_{CPA} - \mathbf{P}_B + \mathbf{P}_A\| = \|(\mathbf{P}_A + \mathbf{v}_A \cdot t_{CPA}) - (\mathbf{P}_B + \mathbf{v}_B \cdot t_{CPA})\| = d_{CPA}$$

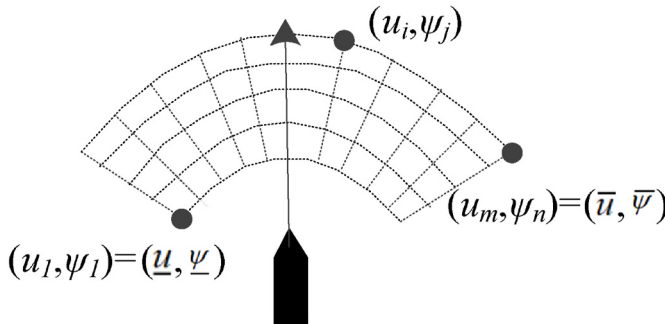


Fig. 6. The discretized velocities acquired by sampling between $[\underline{u}, \underline{\psi}]$ and $[\bar{u}, \bar{\psi}]$.

Furthermore, since $R(\mathbf{P}_B, \mu(\mathbf{P}_A, \mathbf{v}_{AB})) = r_A + r_B \geq d_{\min}$ from (6), therefore d_{CPA} corresponding to this \mathbf{v}_{AB} is greater than or equal to d_{\min} (Kufoalor et al., 2018).

The above analysis can be summarized in the following [Proposition](#).

Proposition. If $\mu(\mathbf{P}_A, \mathbf{v}_{AB})$ is tangent to the circle with the radius $R(\mathbf{P}_B, \mu(\mathbf{P}_A, \mathbf{v}_{AB})) \geq d_{\min}$ and the center \mathbf{P}_B , the d_{CPA} corresponding to \mathbf{v}_{AB} is equal to the radius $R(\mathbf{P}_B, \mu(\mathbf{P}_A, \mathbf{v}_{AB}))$ of this circle, thus $d_{CPA} \geq d_{\min}$.

On the other hand, in Fig. 3, the edge λ_l of CC is the reflection of other edge λ_r with respect to $(\mathbf{P}_B, \mathbf{P}_A)$. In fact, $\mu(\mathbf{P}_A, \mathbf{v}_{AB})$ in Fig. 4 corresponds to an edge λ_r of CC in Fig. 3, thus if choosing a \mathbf{v}_{AB} inside of the CC, then $\mu(\mathbf{P}_A, \mathbf{v}_{AB}) = d_{CPA} < d_{\min}$ and there are collision risks between the vessel A and the vessel B. On the contrary, if choosing a \mathbf{v}_{AB} outside of the CC, that is, choosing a \mathbf{v}_A outside of the $VO_{A|B}$ for the vessel A, then $\mu(\mathbf{P}_A, \mathbf{v}_{AB}) = d_{CPA} \geq d_{\min}$ and definitely collisions will be avoided.

3.3. PVO method and optimal decision-making

Considering the rules 13–15 and the rule 8 of COLREGs, we propose the following four constraints of the changes in course and/or speed of USVs.

- The changes in course and/or speed of USVs should comply with COLREGs.
- The changes in course and/or speed should also meet the kinematic constraints of USVs;
- A series of the small changes in course and/or speed of USVs should be avoided.
- The deviation between the collision avoidance velocity \mathbf{v}_{ca} and the preferred velocity \mathbf{v}_{pref} from the guidance subsystem of USVs should be minimum. In addition, the changes in course should have priority.

In order to obtain better collision avoidance performance of USVs, we improve the traditional VO method by proactively searching for the optimal collision avoidance velocity \mathbf{v}_{ca} which considering the above constraints and outside of the velocity obstacles. The improved VO method is called the PVO. Herein the searching process consists of the following four steps.

Step 1. For the crossing encounter scenario shown in Fig. 3, we divide the velocity space outside of the $VO_{A|B}$ into three areas V_1 , V_2 and V_3 by a dotted line l_1 which is perpendicular to the angle bisector l_2 of the vertex-angle of the cone-like area, as shown in Fig. 5.

If a velocity in V_1 is chosen as the USV's velocity, the USV will move away from the vessel B; if a velocity in V_2 is chosen as the USV's velocity, the USV will bypass the vessel B while seeing the vessel B from its starboard side, which is not complying with the rule 15 of COLREGs; if a velocity in V_3 is chosen as the USV's velocity, the USV will bypass the vessel B while seeing the vessel B from its port side, which is complying

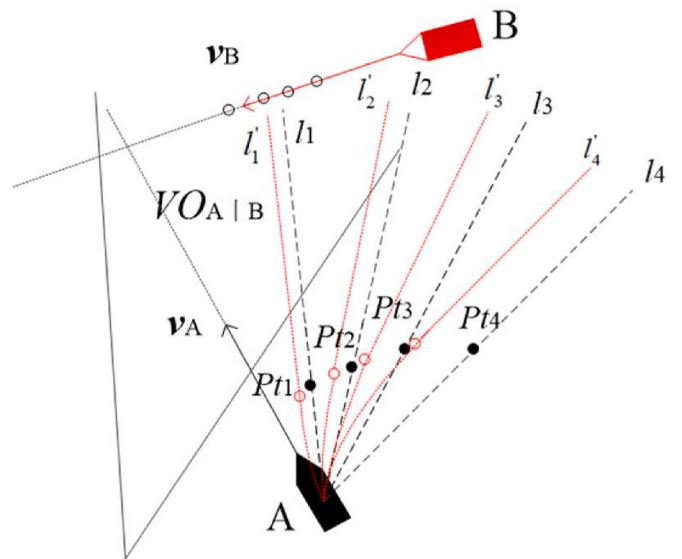


Fig. 7. The schematic diagram of predictive trajectories.

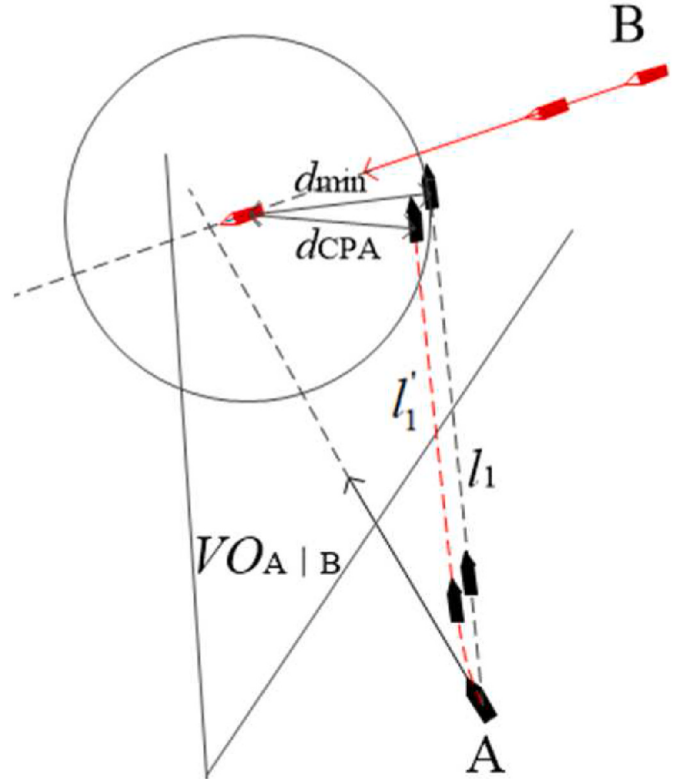


Fig. 8. The schematic diagram of the CPA of two predictive trajectories.

with the rule 15 of COLREGs. Hence we have to search for an optimal \mathbf{v}_{ca} of the USV from V_3 , which satisfies the constraint (i). All velocities which are outside of the velocity obstacles and comply with COLREGs, like the velocities of V_3 , are grouped into a set V_c .

Step 2. Let the feasible speed range of the USV be $[\underline{u}, \bar{u}]$ and the feasible course range of the USV be $[\underline{\psi}, \bar{\psi}]$, where \underline{u} , \bar{u} , $\underline{\psi}$, and $\bar{\psi}$ can be calculated by the following formulas:

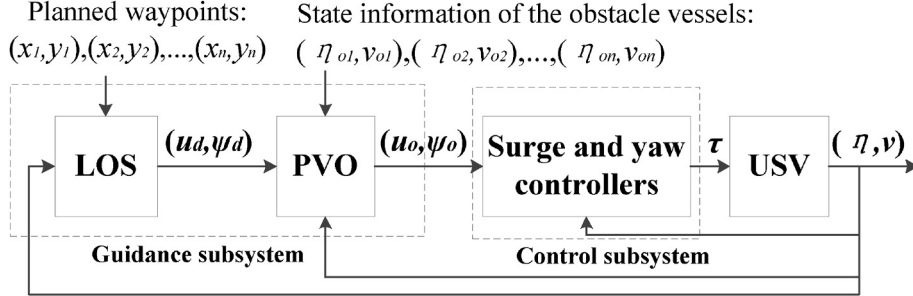


Fig. 9. The schematic of the USV-DCA solution scheme.

$$\begin{cases} \underline{u} = \max(u_{\min}, u_{\text{USV}} - a_{\max} \Delta t) \\ \bar{u} = \min(u_{\max}, u_{\text{USV}} + a_{\max} \Delta t) \\ \underline{\psi} = \psi_{\text{USV}} - r_{\max} \Delta t \\ \bar{\psi} = \psi_{\text{USV}} + r_{\max} \Delta t \end{cases} \quad (10)$$

where u_{USV} and ψ_{USV} denote the current speed and course of the USV, respectively; u_{\min} and u_{\max} denote the minimum and the maximum surge speeds of the USV, respectively; a_{\max} denotes the maximum surge acceleration of the USV; r_{\max} denotes the maximum yaw rate of the USV; Δt represents a period of time from now to some future moment. Hence we have to search for an optimal v_{ca} of the USV within the feasible velocity range, which satisfies the constraint (ii).

Step 3. M speeds are sampled at intervals of N_u m/s in the range $[\underline{u}, \bar{u}]$ and n courses are sampled at intervals of N_ψ radian in the range $[\underline{\psi}, \bar{\psi}]$, as shown in Fig. 6. Therefore we have $m \times n$ speed and course pairs (u_i, ψ_j) , $(i = 1, 2, \dots, m, j = 1, 2, \dots, n)$, and we note $V_l = \{(u_i, \psi_j), i = 1, 2, \dots, m, j = 1, 2, \dots, n\}$. If any (u_i, ψ_j) is in V_c , the speed and course pair, i.e., the velocity satisfies the constraints (i)-(ii) and is outside of the $VO_{A|B}$, which is a candidate velocity that we are searching for.

In order to predict the motion states of the USV, we rewrite the USV's motion mathematical model (1) as follows.

$$\begin{cases} \dot{v} = m^{-1}[\tau - C(v)v - D(v)v] \\ \dot{\eta} = J(\psi)v \end{cases} \quad (11)$$

Then applying Euler method, we have the discrete-time equations of (11) as follows.

$$\begin{cases} v(k+1) = v(k) + TM^{-1}[\tau(k) - C(v(k))v(k) - D(v(k))v(k)] \\ \eta(k+1) = \eta(k) + t[J(\psi(k))v(k+1)] \end{cases} \quad (12)$$

where $x(k) = x(kT)$ and $x(k+1) = x(kT + T)$; T is the sampling period.

If the traditional VO method was employed to solve the collision avoidance problem, assuming that the USV instantaneously accomplishes any desired course change and sails at a new course and current speed, we can obtain the linear predictive trajectories, i.e. the black dotted lines $l_1, l_2, l_3, l_4 \dots$ shown in Fig. 7, by the following equations

$$\begin{cases} x(t) = x(t_c) + u_c \cos(\psi_c)(t - t_c) \\ y(t) = y(t_c) + u_c \sin(\psi_c)(t - t_c) \end{cases} \quad (13)$$

where t_c represents the current moment and (u_c, ψ_c) is the corresponding speed and course pair of the USV at the moment t_c .

However, course and/or speed changes of the USV need to cost some time due to the dynamic characteristics of the USV. If considering the dynamics of the USV, we can obtain the nonlinear predictive trajectories, i.e., the red dotted lines $\hat{l}_1, \hat{l}_2, \hat{l}_3, \hat{l}_4 \dots$ shown in Fig. 7 by the discrete-time equation (12). t_i ($i = 1, 2, 3, 4 \dots$) represents the moment at which the USV accomplishes the i th desired course change, and P_{ti} is the corresponding position of the USV at the moment t_i . It is seen from Fig. 7 that at the moment t_i , the positions of the USV on a red dotted line \hat{l}_1 and

a black line \hat{l}_1 are not same, and the greater the course change of the USV is, the greater the position deviation is. Therefore, the optimal decision-making v_{ca} in the current decision-making period may fall into the velocity obstacle in the next period, which thus will cause a series of small course and/or speed changes of the USV. This problem can be intuitively analyzed by using the CPA parameters in Section 3.2.

As shown in Fig. 8, l_1 and \hat{l}_1 are different predictive trajectories corresponding to the optimal decision-making v_{ca} obtained by the traditional VO method in the current period. If we calculate the minimum distance d_{CPA} between the vessels A and B, we can find that d_{CPA} is less than the safe distance d_{\min} when the USV sails along \hat{l}_1 and arrives at the CPA, as shown in Fig. 8. Then this v_{ca} is not the optimal collision avoidance velocity in the current period.

In order to avert a series of small course and/or speed changes of the USV, we first predict the position of the USV at the moment t_i by (12), and the position of any obstacle vessel at t_i can be linearly predicted by (13). Let $P_{t_i}^{\text{USV}}$ represent the predictive position of the USV at the moment t_i , $P_{t_i}^{Oj}$ represent the predictive position of the j th obstacle vessel at the moment t_i , and $d(P_{t_i}^{\text{USV}}, P_{t_i}^{Oj})$ denote the distance between $P_{t_i}^{\text{USV}}$ and $P_{t_i}^{Oj}$. If the distance between the USV and any one of its obstacle vessels at the moment t_i satisfies

$$d(P_{t_i}^{\text{USV}}, P_{t_i}^{Oj}) \leq d_{\min} \quad (14)$$

there are collision risks between the USV and its obstacle vessels.

Then we calculate the time to CPA $t_{\text{CPA}}^{\text{USV}-Oj}$ and the distance at CPA $d_{\text{CPA}}^{\text{USV}-Oj}$ of the USV and its j th obstacle vessel by equation (4) according to the predictive positions and velocities of the USV and its obstacle vessels at the moment t_i . Therefore we can pre-judge whether there are collision risks between the USV and any one of its obstacle vessels by follows

$$0 \leq t_{\text{CPA}}^{\text{USV}-Oj}(t_i) \leq t_{\max} \text{ and } d_{\text{CPA}}^{\text{USV}-Oj}(t_i) \leq d_{\min} \quad (15)$$

if (15) is satisfied, there are collision risks between the USV and its obstacle vessels.

In this way, from the candidate velocities, we can screen out some velocities which satisfy (14)–(15) and cause collision risks.

Step 4. We search for an optimal v_{ca} satisfying the conditions (iii)–(iv) from the candidate velocities by the following cost function

$$C = \alpha(u_i - u_d)^2 + \beta(\psi_j - \psi_d)^2 + \gamma f_{\text{CPA}}^{(u_i, \psi_j)} \quad (16)$$

where u_d is the desired speed and ψ_d is the desired course; $f_{\text{CPA}}^{(u_i, \psi_j)}$ is a Boolean function; α, β, γ are weight coefficients.

u_d and ψ_d are obtained by the LOS module of the guidance subsystem. LOS is a commonly used method for path following, and for more details, readers can refer to Section 4.3. $f_{\text{CPA}}^{(u_i, \psi_j)}$ can be determined by judging whether the parameters satisfy equations (14) and (15). If they satisfy (14) and (15), the value of $f_{\text{CPA}}^{(u_i, \psi_j)}$ is 1; otherwise, the value of $f_{\text{CPA}}^{(u_i, \psi_j)}$ is 0. In order to satisfy the constraints (iii)–(iv), there should be $\gamma > \alpha > \beta$.

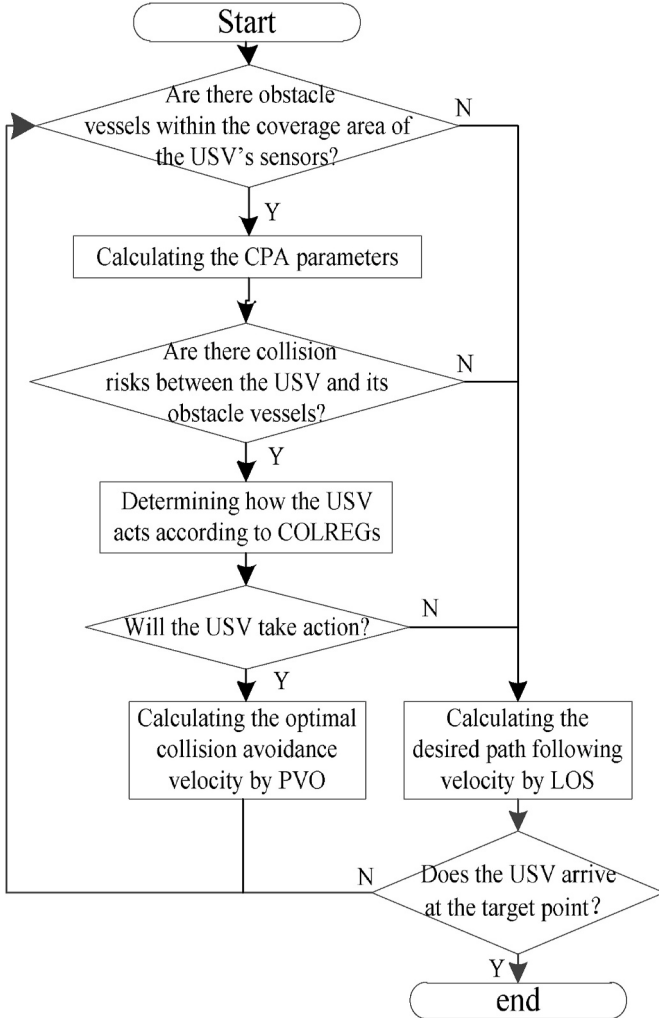


Fig. 10. The decision-making process flow chart of the USV-DCA solution scheme.

3.4. The searching process of the PVO method

The main steps of the PVO method are summarized as follows.

- Judging whether there are collision risks between the USV and the obstacle vessels within the coverage area of the USV's sensors. Please refer to equations (4) and (5) in Section 3.2.
- Constructing the velocity obstacles based on the positions and velocities of the USV and its obstacle vessels when the USV should take actions to avoid collision. Please refer to equations (8) and (9) in Section 3.2.
- Finding a set of velocities V_c of the USV, which complies with COLREGs and is outside of the velocity obstacles. Please refer to Step 1 in Section 3.3.
- Obtaining a set of the feasible discretized velocities V_l according to the kinematic constraints of the USV and the candidate velocities by $V_c \cap V_l$. Please refer to Step 1 and Step 2 in Section 3.3.
- Searching for an optimal v_{ca} from the candidate velocities by means of the cost function (16) in Section 3.3.

Remark 1. Compared with the VO method, the PVO method can avert a series of small course and/or speed changes of the USV, therefore it can make the USV avoid frequent velocity corrections at the beginning of collision avoidance and reduce wear and tear of actuators. In the face of

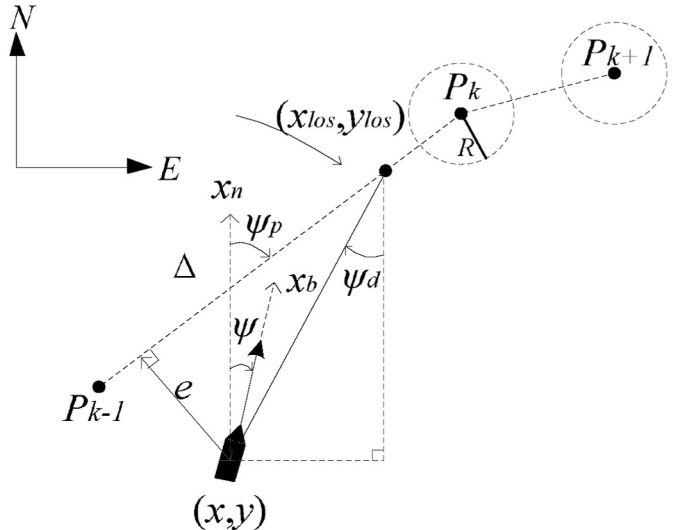


Fig. 11. The schematic diagram of the path following with the LOS method.

some emergency collision avoidance situations, such as the situation that obstacle vessels suddenly appear in the area near the USV, the PVO method can enable the USV to make faster course and/or speed adjustment in advance, thus the USV makes safer collision avoidance actions. In addition, our proposed PVO method by improving the cost function of the VO method keeps the VO's good mathematical qualities, i.e., simple to compute and easy to adapt and tune for different collision avoidance requirements.

4. USV-DCA solution scheme

4.1. The principle and the decision-making process of USV-DCA solution scheme

In order to solve the limitations of the SRF collision avoidance method in the original SBG framework in the case of multiple vessels encounter, we design a guidance and control system of the USV by integrating the proposed PVO method and the LOS method into the SBG framework, and present a USV-DCA solution scheme whose working principle diagram is shown in Fig. 9 based on the PVO method and the SBG framework.

The planned waypoints in Fig. 9 are provided by the global path planning algorithm and the motion states information of the obstacle vessels in Fig. 9 is provided by the onboard camera, radar or AIS system. According to the planned waypoints and the current motion states of the USV, the LOS module calculates a path following speed and course pair (u_d, ψ_d) . According to the (u_d, ψ_d) and the current motion states of the USV and its obstacle vessels, the PVO module calculates an optimal collision avoidance speed and course pair (u_o, ψ_o) , which is sent to the control subsystem if there exist collision risks between the USV and its obstacle vessels. These two modules construct the guidance subsystem of the USV. By constantly measuring the USV's speed and course and comparing it to the desired (u_o, ψ_o) , the control subsystem consisting of surge and yaw controllers can determine the velocity error and calculate the required control force and moment to minimize the velocity error of the USV. Under the actuation of the calculated control force and moment, then the USV can navigate along the desired path while avoiding collisions with other obstacle vessels.

The decision-making process of this solution scheme is shown in Fig. 10. At the beginning of the USV's navigation, there are generally no obstacle vessels around the USV.

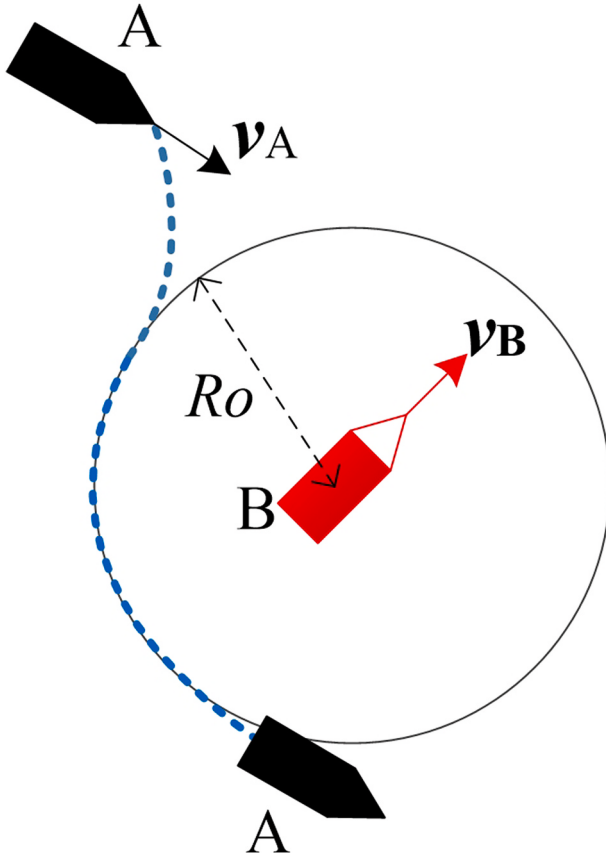


Fig. 12. The schematic diagram of a crossing encounter case.

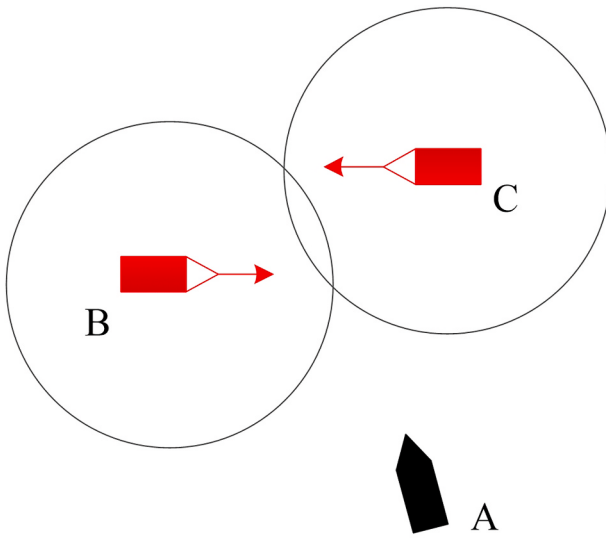


Fig. 13. The schematic diagram of a multi-vessel-encounter case.

4.2. LOS method

Fig. 11 illustrates the principle of the LOS method, where P_{k-1} , P_k , P_{k+1} are the planned waypoints of the USV; (x, y) is the current position of the USV; ψ is the current course of the USV; $(x_{\text{los}}, y_{\text{los}})$ is the LOS guidance point and is determined by a predefined look-ahead distance Δ which is usually 3–5 times the length of the USV; ψ_d is the desired course of the USV and is calculated by

Table 1
Parameters of the USV.

parameter	value	unit
m_{11}	3980.0	Kg
m_{22}	3980.0	Kg
m_{33}	19703.0	kg/m^2
d_{u1}	-50.0	kg/m^2
d_{v1}	-200.0	kg/m^2
d_{r1}	-3224.0	$\text{kg}\cdot\text{m}^2/\text{s}$
$d_{u2 u }$	-135.0	kg/m^2
$d_{v2 v }$	-2000.0	kg/s^2
$d_{r3 r ^2}$	-3224.0	$\text{kg}\cdot\text{m}^2/\text{s}$

Table 2
Design parameters of the guidance subsystem and controllers.

parameter	value	parameter	value
R	8 m	α	8
t_{\max}	50s	β	4
d_{\min}	20 m	γ	20
\bar{u}	8 m/s	Δ	40 m
\underline{u}	0 m/s	R	10 m
$\bar{\psi}$	1.57 rad	K_{pu}	0.1s^{-1}
$\underline{\psi}$	-1.57 rad	$K_{p\psi}$	5.0s^{-1}
T	0.1s	$K_{d\psi}$	1s

$$\psi_d = \psi_p + \arctan\left(\frac{-e}{\Delta}\right) \quad (17)$$

where ψ_p is the angle between the north direction and the straight line $P_{k-1}-P_k$; e is the path cross-track error.

Note that the course deviation $\psi_e = \psi_d - \psi$. If ψ_e tends to 0, the USV can follow the desired path.

In order to judge whether the USV has arrived at the desired path point, we assume that there exists an acceptance circle (Oh and Sun, 2010), whose center is the current desired path point P_k and radius is R . If the distance between the current position (x, y) of the USV and the position (x_k, y_k) of the current desired path point P_k satisfy

$$(x_k - x)^2 + (y_k - y)^2 \leq R^2 \quad (18)$$

then the USV will arrive at the path point P_k and sail to the next path point P_{k+1} .

4.3. Surge and yaw controllers

The surge proportional controller and yaw proportional-derivative controller are given as follows, respectively (Myre, 2016).

$$\begin{cases} \tau_u = -(m_{22}v + m_{23}r)r - \left(X_{u1} + \sum_{u=2}^3 X_{ui}|u|^{i-1}\right)u + k_{pu}(u_d - u) \\ \tau_r = k_{p\psi}m_{33}((\psi_d - \psi) + k_{d\psi}(\dot{\psi}_d - \dot{\psi})) \end{cases} \quad (19)$$

where K_{pu} and $K_{p\psi}$ are proportional gains and $K_{d\psi}$ is the derivative gain.

Remark 2. The SBG framework consists of the LOS and the SRF

Table 3
Initial states and target point information.

Encounter scenario	vessel	Initial point (x_0, y_0)	course ψ	surge speed u	Target point (x_g, y_g)
Head-on	USV	(-100,100)	0 rad	4 m/s	(100,100)
	OV	(100,100)	$-\pi$ rad	3 m/s	-
Overtaking	USV	(-100,100)	0 rad	4 m/s	(100,100)
	OV	(-70,100)	0 rad	2 m/s	-
Crossing	USV	(-100,100)	0 rad	4 m/s	(100,100)
	OV	(50,50)	0.75 π rad	3 m/s	-

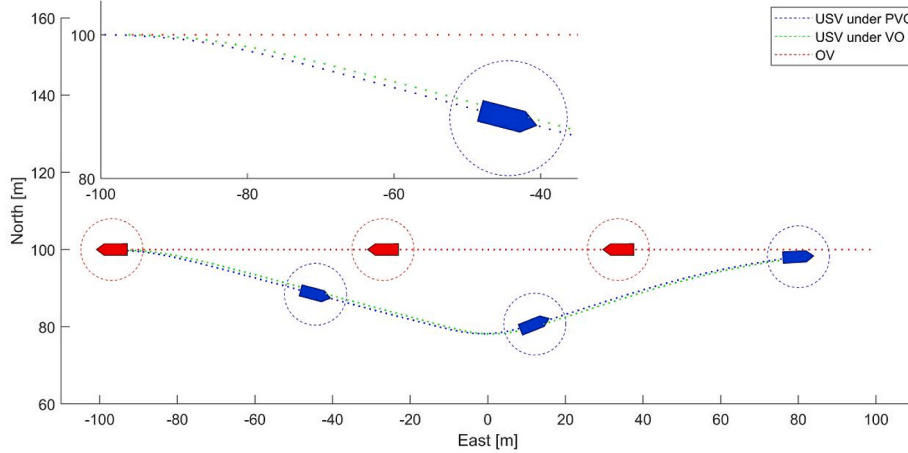


Fig. 14a. The simulation results in the head-on encounter scenario. (a) Collision avoidance trajectories.

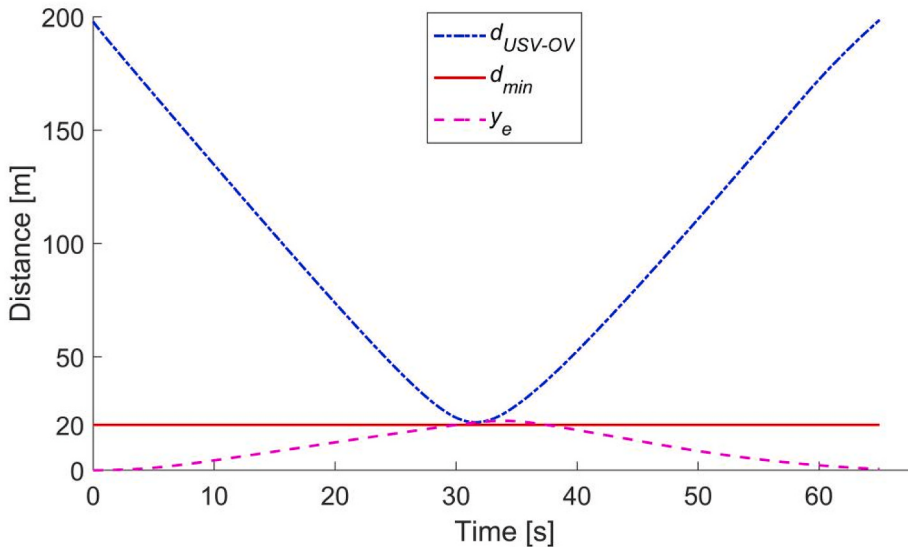


Fig. 14b. The simulation results in the head-on encounter scenario. (b) Distance between the USV and OV and path cross-track error y_e .

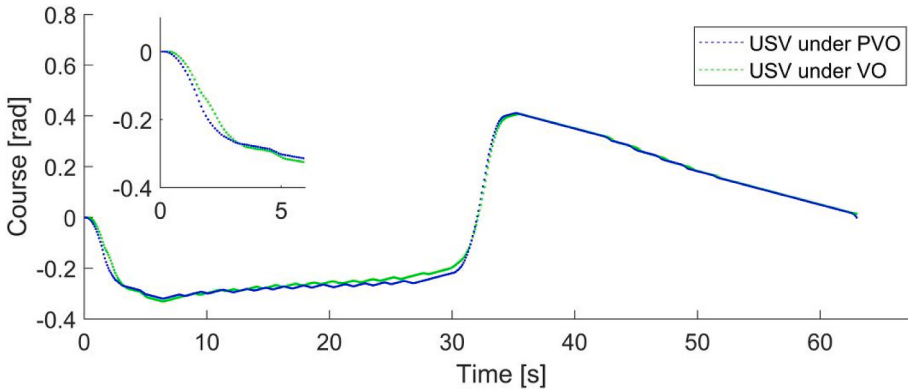


Fig. 14c. The simulation results in the head-on encounter scenario. (c) Course changes of the USV.

methods. The LOS module provides a desired heading for path following and the SRF module provides a desired heading for collision avoidance. The LOS and the SRF methods in the SBG framework switches according to the distance between two vessels. Therein the SRF method is the key to ensure the safe navigation of the USV. Consider the crossing encounter scenarios shown in Fig. 12, where R_o represents the radius of a

safe vessel domain of the obstacle vessel B. The principle of the SRF collision avoidance method is to make the USV keep a safe distance of the radius R_o around the obstacle vessel's center to avoid collisions (Moe and Petersen, 2016). However, the SRF collision avoidance method in the SBG framework only deals with one obstacle vessel at a time and does not consider the problem of overlapping obstacles in the case of

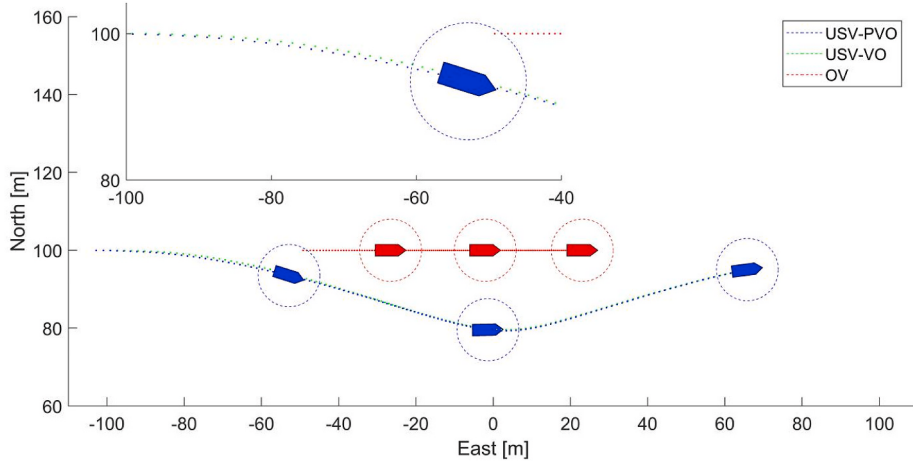


Fig. 15a. The simulation results in the overtaking scenario. (a) Collision avoidance trajectories.

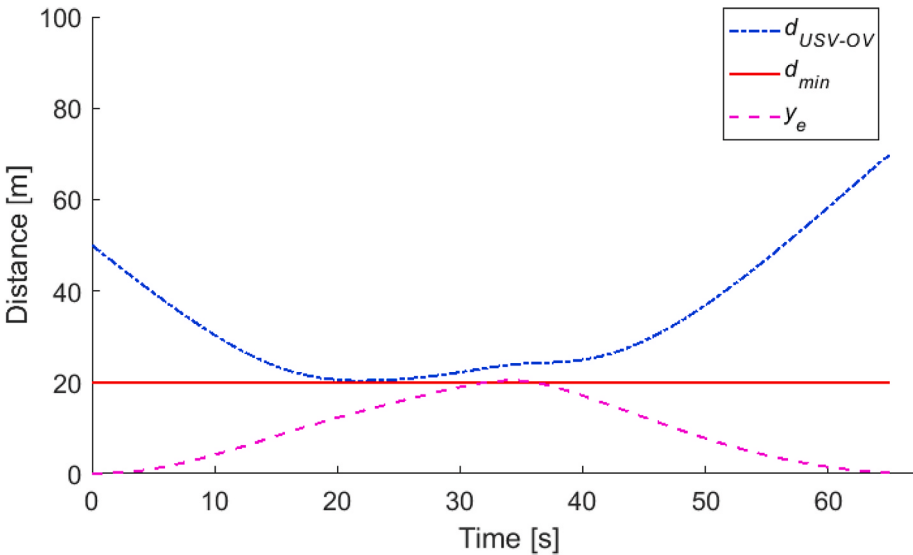


Fig. 15b. The simulation results in the overtaking scenario. (b) Distance between the USV and OV and path cross-track error y_e .

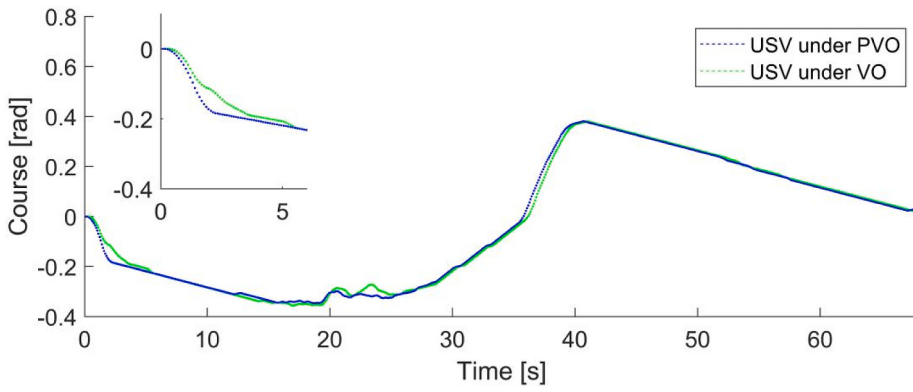


Fig. 15c. The simulation results in the overtaking scenario. (c) Course changes of the USV.

multiple vessels encounter (Moe and Pettersen, 2016), as shown in Fig. 13. As such, it might make an unsafe collision avoidance decision for the USV when the overlapping obstacles appear. Our proposed PVO method can deal with the overlapping obstacles problem by constructing multiple velocity obstacles, such that our proposed USV-DCA solution

scheme based on the LOS and the PVO methods can still make a reasonable and safe collision avoidance decision even in the case of overlapping obstacle.

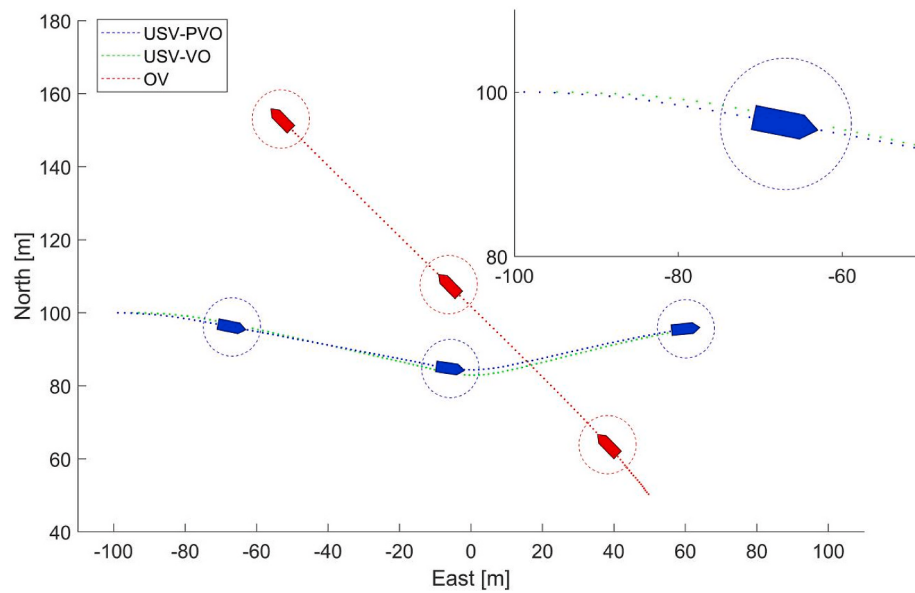


Fig. 16a. The simulation results in the crossing scenario. (a) Collision avoidance trajectories.

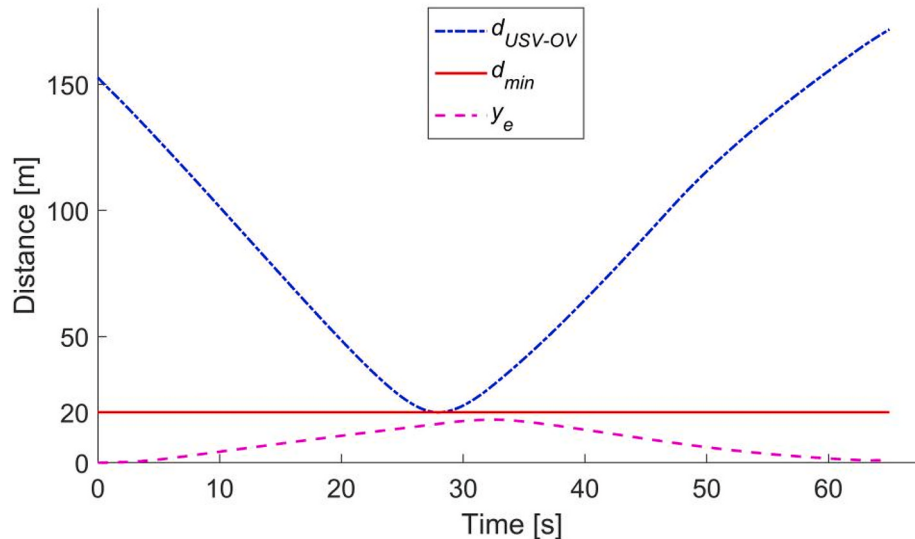


Fig. 16b. The simulation results in the crossing scenario. (b) Distance between the USV and OV and path cross-track error y_e .

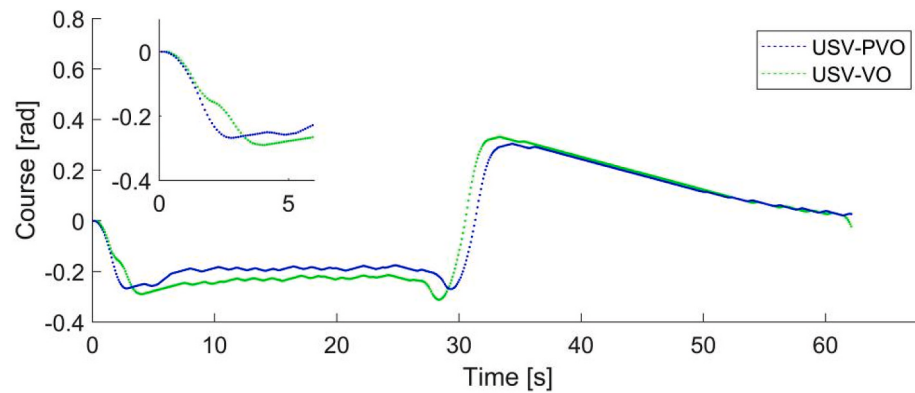


Fig. 16c. The simulation results in the crossing scenario. (c) Course changes of the USV.

Table 4
Initial states and target point information.

	USV	OV1	OV2
Initial point (x_0, y_0)	(0,0)	(130,20)	(50,50)
course ψ	0.25π rad	0.75π rad	0.21π rad
surge speed u	5 m/s	3 m/s	1 m/s
target point	(140,140)	-	-

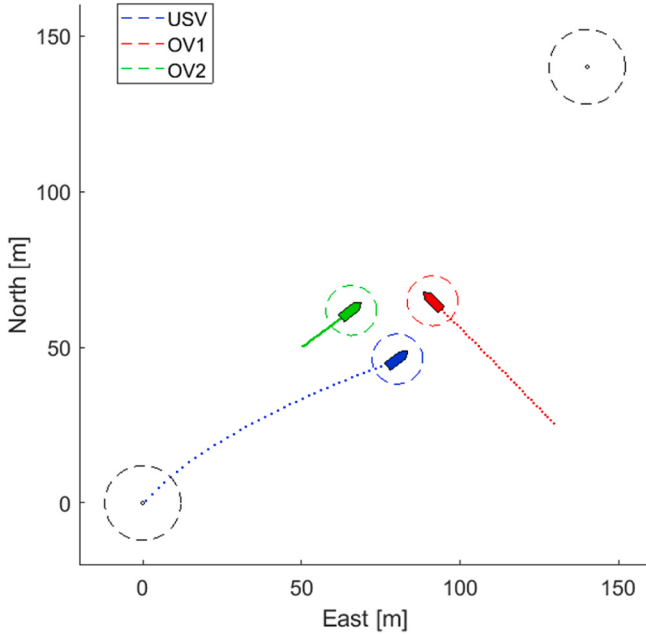


Fig. 17a. The simulation results in the multiple vessels encounter case under the USV-DCA solution scheme. (a) Collision avoidance trajectories ($t=20$ s).

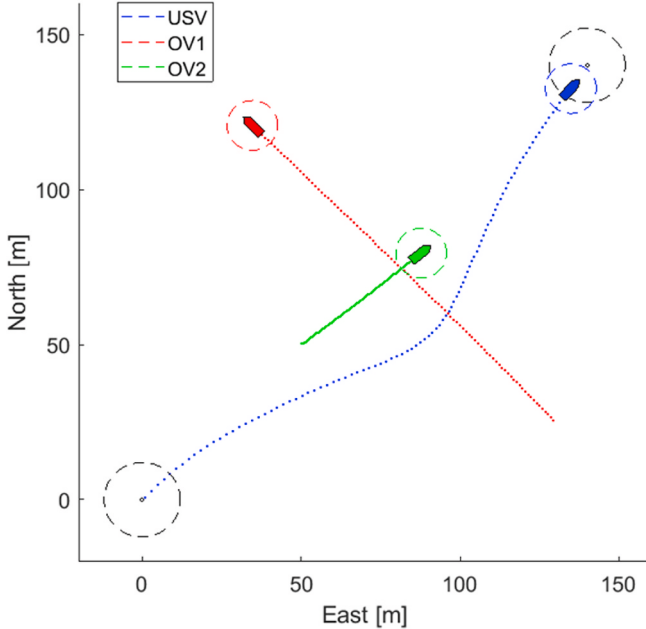


Fig. 17b. The simulation results in the multiple vessels encounter case under the USV-DCA solution scheme. (b) Collision avoidance trajectories ($t=49$ s).

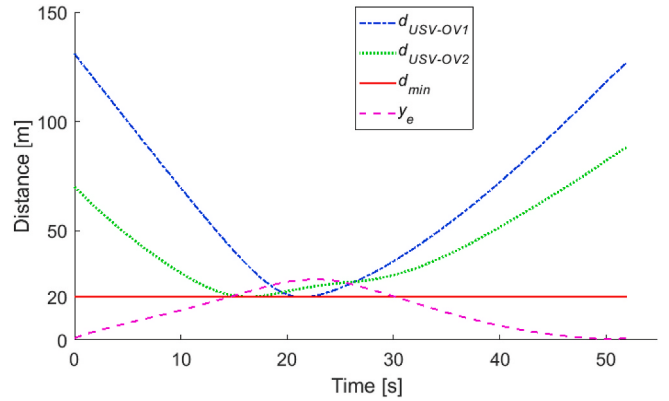


Fig. 17c. The simulation results in the multiple vessels encounter case under the USV-DCA solution scheme. (c) Distances between the USV and obstacle vessels and path cross-track error y_e .

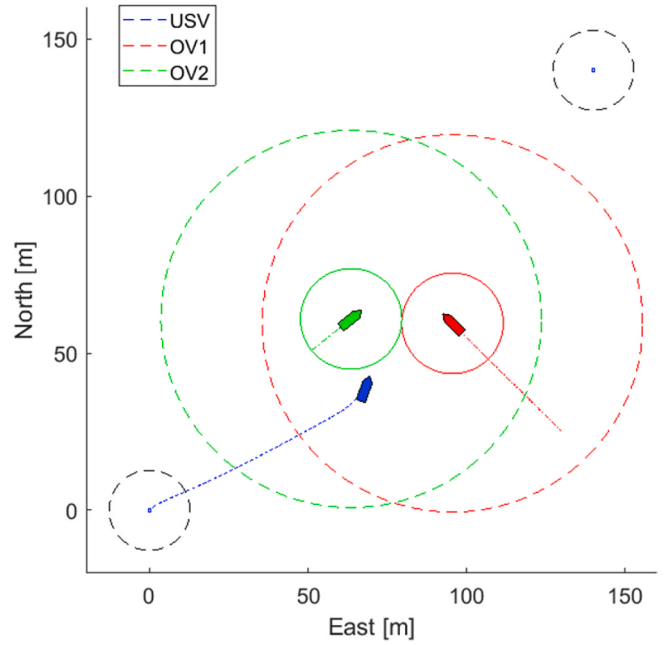


Fig. 18a. The simulation results in the multiple vessels encounter case under the original SBG framework. (a) Collision avoidance trajectories ($t=14$ s).

5. SIMULATION results

In order to verify the effectiveness and superiority of our proposed USV-DCA solution scheme based on the PVO and the SBG framework, we carry out the simulations on a USV in the cases of single vessel encounters and multiple vessels encounters using Matlab/Simulink and the ROS system. In the simulations, we use the vessel motion mathematical model (1) with parameters shown in Table 1 (Myre, 2016), and the design parameters of the guidance subsystem and controllers are taken as shown in Table 2.

Single vessel encounter case: In order to verify the superiority of the USV-DCA solution scheme with the PVO method to that with the traditional VO method in collision avoidance decision-making, we carry out the simulations in the three cases that the USV encounters with a single obstacle vessel in the head-on, overtaking and crossing scenarios. The initial motion states of and the obstacle vessel (OV) and the USV's target point are set in Table 3.

The simulation results under the USV-DCA solution scheme in the head-on, overtaking and crossing encounter scenarios are shown in

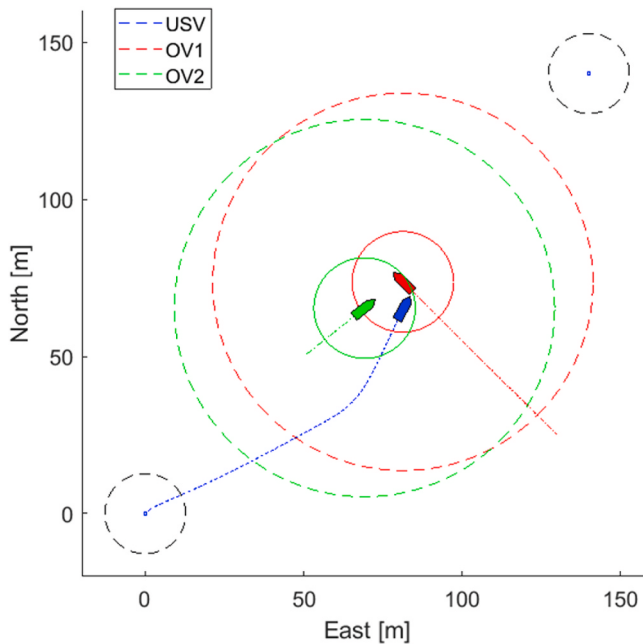


Fig. 18b. The simulation results in the multiple vessels encounter case under the original SBG framework. (b) Collision avoidance trajectories ($t=22s$).

Figs. 14–16, respectively.

It is seen from Figs. 14(a) and 15(a) and 16(a) that in the three encounter scenarios, the USV-DCA solution scheme can make the USV successfully avoid the obstacle vessel complying with COLREGs and follow the desired straight line path without collisions. Figs. 14(b) and 15(b) and 16(b) show that in the three encounter scenarios, the distance between the USV and the OV is always greater than or equal to the safe distance d_{\min} , and the path cross-track error y_e tends to 0 when there are no collision risks between the USV and the OV, which is consistent with the objectives of collision avoidance in this paper. Furthermore, Figs. 14(a) and 15(a) and 16(a) show that in the three encounter scenarios, the blue dotted line trajectories are below the green dotted line trajectories in the initial segments of the USV's trajectories with collision avoidance. Figs. 14(c) and 15(c) and 16(c) exhibit that all the courses in the initial segments of the USV's course curves in the three encounter scenarios change faster under the USV-DCA solution scheme with the PVO method than under the USV-DCA solution scheme with the VO method. Therefore, we can determine that the USV under the USV-DCA solution scheme with the PVO method sails in a direction of avoiding obstacle vessel earlier than under the USV-DCA solution scheme with the traditional VO method. This is because the PVO method can pre-judge whether there are collision risks according to the predicted motion states of the USV, so that the USV can make a better collision avoidance decision in advance and avert a series of small course and/or speed changes.

Multiple vessels encounter case: In order to further verify the superiority of our proposed USV-DCA solution scheme to the original SBG framework, we carry out the simulations in the case that the USV encounters with two obstacle vessels. The initial motion states of the USV and its obstacle vessels (OV1 and OV2) and USV's target point are set as shown in Table 4.

The simulation results under the USV-DCA solution scheme and the original SBG framework are shown in Fig. 17 and Fig. 18, respectively.

As shown in Fig. 17(a) and (b), the USV under the USV-DCA solution scheme successfully avoids OV1 and OV2 complying with COLREGs and follows the desired straight line path without collisions, which is because the PVO method can construct velocity obstacles for different obstacle vessels at the same time and find the optimal collision avoidance velocity outside the total velocity obstacle. Fig. 17(c) shows that in

the multiple vessels encounter case, distances between the USV and the obstacle vessels are always greater than or equal to the safe distance d_{\min} , and the path cross-track error y_e tends to 0 when there are no collision risks between the USV and the obstacle vessels, which is consistent with the objectives of collision avoidance in this paper. However, it is seen from Fig. 18(a) that when the vessel domains of the two obstacle vessels intersect, the USV under the original SGB framework suddenly sails to the left, which leads to a collision between the USV and OV1 at the moment 22s as shown in Fig. 18(b). This indicates that in the multiple vessels encounter case, the original SBG framework makes a wrong collision avoidance decision for the USV when the vessel domains of the obstacle vessels intersect.

6. Conclusions

In this paper, in order to solve the USVs' dynamic collision avoidance problem, we innovatively proposed the PVO method which can pre-judge whether there are collision risks according to the predicted motion states of USVs by the vessel motion mathematical model, and then create a USV-DCA solution scheme by integrating the PVO method and the LOS method into the original SBG framework. Finally, we carry out simulations in the cases of single vessel and multiple vessels encounter to verify the effectiveness and superiority of our proposed USV-DCA solution scheme. The simulation results show that our created USV-DCA solution scheme can make USVs avert a series of small velocity changes and performs better than the original SBG framework in collision avoidance decision-making in the multiple vessels encounter case. Thus the proposed USV-DCA solution scheme increases the safety of USVs' collision avoidance process. Also it can be extended to other unmanned systems. In the future, we will further research whether our PVO method in the USV-DCA solution scheme can be applied to the situation that other obstacle vessels also have the same collision avoidance function, and we will research how to make collision avoidance decisions in the presence of ocean environmental disturbances.

CRediT authorship contribution statement

Wang Wenming: Investigation, Writing – original draft, Visualization. **Du Jialu:** Conceptualization, Methodology, Writing – review & editing, Supervision, Funding acquisition. **Tao Yihan:** Writing – review & editing.

Declaration of competing interest

The authors declare that they have no known competing financial interests or personal relationships that could have appeared to influence the work reported in this paper.

References

- Alonso-Mora, J., Breitenmoser, A., Beardsley, P., Siegwart, R., 2013a. Reciprocal collision avoidance for multiple car-like robots. In: 2013 IEEE International Conference on Robotics and Automation (ICRA). IEEE, Saint Paul, MN, USA, pp. 360–366.
- Alonso-Mora, J., Breitenmoser, A., Rufli, M., Beardsley, P., Siegwart, R., 2013b. Optimal Reciprocal Collision Avoidance for Multiple Non-holonomic Robots, vol. 83. Springer Tracts in Advanced Robotics, pp. 203–216.
- Berg, J.P.V.D., Lin, M.C., Manocha, D., 2008. Reciprocal velocity obstacles for real-time multi-agent navigation. In: IEEE International Conference on Robotics and Automation (ICRA). IEEE, Pasadena, California, USA, pp. 1928–1935.
- Cheng, Y., Sun, Z., Huang, Y., Zhang, W., 2019. Fuzzy categorical deep reinforcement learning of a defensive game for an unmanned surface vessel. Int. J. Fuzzy Syst. 21 (2), 592–606.
- Fiorini, P., Shiller, Z., 1998. Motion planning in dynamic environments using velocity obstacles. Int. J. Robot Res. 17 (7), 760–772.
- Fossen, T.I., 2011. Handbook of Marine Craft Hydrodynamics and Motion Control. Norwegian University of Science and Technology, Trondheim, Norway.
- Fox, D., Burgard, W., 1997. The dynamic window approach to collision avoidance. IEEE Robot. Autom. Mag. 4 (1), 23–33.
- IMO, 1972. Convention on the International Regulations for Preventing Collisions at Sea (COLREGs).

- Khatib, O., 1986. Real-time obstacle avoidance system for manipulators and mobile robots. *Int. J. Robot Res.* 5 (1), 90–98.
- Kluge, B., Prassler, E., 2004. Reflective navigation: individual behaviors and group behaviors. In: *IEEE International Conference on Robotics & Automation*. IEEE, New Orleans, LA, USA, pp. 4172–4177.
- Kufoalor, D., Brekke, E.F., Johansen, T.A., 2018. Proactive collision avoidance for ASVs using a dynamic reciprocal velocity obstacles method. In: *IEEE/RSJ International Conference on Intelligent Robots and Systems (IROS)*. IEEE, Madrid, Spain, pp. 2402–2409.
- Kuwata, Y., Wolf, M.T., Zarzhitsky, D., Huntsberger, T.L., 2014. Safe maritime autonomous navigation with COLREGS, using velocity obstacles. *IEEE J. Ocean. Eng.* 39 (1), 110–119.
- Loe, Ø.A.G., 2008. Collision Avoidance for Unmanned Surface Vehicles. Master's thesis. Norwegian University of Science and Technology, Trondheim, Norway.
- Ministry of Industry and Information Technology, 2019. The execution plan for the development of intelligent ships (2019-2021). *Ship Stand. Eng.* 52 (1), 7–10.
- Moe, S., Pettersen, K.Y., 2016. Set-based Line-of-Sight (LOS) path following with collision avoidance for underactuated unmanned surface vessel. In: 24th Mediterranean Conference on Control and Automation (MED). IEEE, Athens, Greece, pp. 402–409.
- Myre, H., 2016. Collision Avoidance for Autonomous Surface Vehicles Using Velocity Obstacle and Set-Based Guidance. Master's thesis, Norwegian University of Science and Technology, Trondheim, Norway.
- Naeem, W., Henrique, S.C., Hu, L., 2016. A reactive COLREGs-compliant navigation strategy for autonomous maritime navigation. *IFAC-PapersOnLine* 49 (23), 207–213.
- Oh, S.R., Sun, J., 2010. Path following of underactuated marine surface vessels using line-of-sight based model predictive control. *Ocean Eng.* 37 (2–3), 289–295.
- Sandbakken, J.E., 2018. Collision Avoidance for Autonomous Ships in Transit. Master's thesis. Norwegian University of Science and Technology, Trondheim, Norway.
- Song, A.L., Su, B.Y., Dong, C.Z., Shen, D.W., Xiang, E.Z., Mao, F.P., 2018. A two-level dynamic obstacle avoidance algorithm for unmanned surface vehicles. *Ocean Eng.* 170 (15), 351–360.
- Xu, X., Pan, W., Huang, Y., Zhang, W., 2020. Dynamic collision avoidance algorithm for unmanned surface vehicles via layered artificial potential field with collision cone. *J. Navig.* 73 (6), 1306–1325.
- Zhao, Y., Li, W., Shi, P., 2016. A real-time collision avoidance learning system for unmanned surface vessels. *Neurocomputing* 182, 255–266.